

THE ALKALI FELDSPARS OF THE TATOOSH PLUTON  
IN MOUNT RAINIER NATIONAL PARK<sup>1</sup>

THOMAS L. WRIGHT, *U. S. Geological Survey, Hawaiian  
Volcano Observatory, Hawaii*

ABSTRACT

Twenty-five orthoclase microperthites from a shallow intrusion of granodiorite-quartz monzonite have been studied chemically, optically and by  $x$ -ray diffraction. The data presented are: bulk composition; composition and obliquity of the potassium-rich phase;  $\alpha^*$  and  $\gamma^*$  for the sodium-rich phase;  $2V$  for both potassium-rich and sodium-rich phases.  $2V$  of each phase is correlated with the composition of that phase on a  $2V$ -composition diagram. Plotting  $2V$  of perthites opposite the bulk composition should be abandoned.

The potassic phases of the perthites are structurally intermediate between orthoclase and maximum microcline; average  $2V_x$  and obliquity of this phase increase with decreasing Ab content. The sodic phases are intermediate between high and low albite;  $2V_x$  increases with the size of the exsolution lamellae in individual crystals and  $\gamma^*$  measured for the sodic phase is higher (closer to low albite), in specimens showing more exsolution. Thus both phases of the perthites exhibit a continuous inversion from a high to low structural state during exsolution.

The related processes of exsolution and inversion are discussed in terms of two models of the alkali feldspar solvus. Both models indicate that exsolution, if carried to completion, will result in a perthite consisting of maximum microcline and low albite.

INTRODUCTION

Orthoclase microperthites from the Tatoosh pluton, a shallow intrusion of granodiorite-quartz monzonite, have been studied by  $x$ -ray and optical methods. The Tatoosh pluton is in Mount Rainier National Park, Washington (Fig. 1). Only the southern part of the pluton has been studied in detail and all the alkali feldspars were collected from this part. Because of the rapid cooling history of the pluton various stages of exsolution are preserved in the perthites. The purpose of this paper is to give data relating to the orthoclase-microcline inversion and the structural transformations in the sodic phase of the perthites, along with the implications of these data regarding the nature of the exsolution process in alkali feldspars.

PETROLOGY

A detailed study is being made of the petrogenesis of the southern half of the Tatoosh pluton; therefore only a brief summary is given here. The Tatoosh pluton intruded a layered sequence of slightly metamorphosed lower Tertiary volcanic rocks. Country rock is exposed adjacent to the vertical walls of the pluton and in remnants of an original flat-lying roof. A contact aureole in which the country rock is converted to hornfels, extends outward from the pluton for a distance of 1000-4000

<sup>1</sup> Publication authorized by the Director, U. S. Geological Survey.

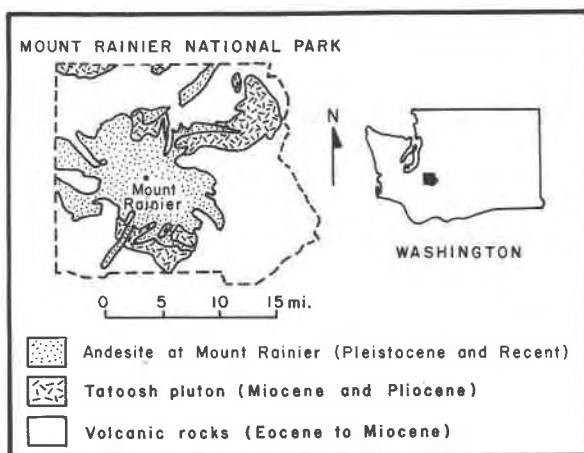


FIG. 1. Index map showing location of the Tatoosh pluton.

feet. The contact between pluton and country rock is sharp and highly discordant. No flow foliation or lineation is present in the plutonic rocks, even adjacent to the contact with country rock. The structural data and the hypidiomorphic granular texture of the granitoid rocks are taken as proof of igneous origin for the pluton. Evidence for chilling and devolatilization of the magma and the Tertiary age of the pluton strongly suggest a shallow depth of emplacement.

The southern part of the pluton has been subdivided into two major units: quartz monzonite and granodiorite. A fine-grained sheath of quartz monzonite, in contact with the country rocks of the roof remnants and the eastern border of the pluton, grades downward and to the west to a medium-grained granodiorite. A chill zone of distinctly porphyritic quartz monzonite extends to a depth of 500 feet below the roof remnants. The coarsest rocks of the pluton (av. grain size = 1.5 mm) are found in the deepest exposures of the granodiorite, about 2500 feet below the roof. Two modes, typical of the rocks of the southern part of the pluton, are shown in Table 1.

Endomorphous alteration has affected the quartz monzonite sheath more than the granodiorite core. The alteration is manifested in saussuritization of plagioclase, clay alteration of alkali feldspar, and chloritization of biotite. There is also a greater amount of exsolution in the alkali feldspars of the quartz monzonite than in those of the granodiorite.

#### STUDY OF THE ALKALI FELDSPARS

*Petrography.* The order of crystallization of the felsic minerals, shown by their mutual textural relations, is plagioclase followed by alkali feldspar followed by quartz.

The plagioclase is complexly zoned from oscillatory cores of composition  $An_{35-45}$  to normally zoned rims of composition  $An_{25-15}$ . The structural state of all such zones is intermediate, as determined on the universal stage (Slemmons, 1962). Rarely, unzoned cores of composition  $An_{50-55}$  and low structural state are found inside the sequence of oscillatory zones.

The alkali feldspar commonly forms blocky crystals, 0.5–1.0 mm in longest dimension, which are in places coarsely intergrown with quartz. Most crystals have a clear extinction and are either untwinned or are twinned on the Carlsbad law. Grid twinning is absent and wavy extinction is rare. All the alkali feldspar is visibly perthitic in thin section and

TABLE 1. MODAL COMPOSITION OF ROCKS FROM THE SOUTHERN PART OF THE TATOOSH PLUTON (VOL. %)

Mineral	Rock Unit	
	Quartz Monzonite	Granodiorite
Quartz	23.4	23.4
Alkali feldspar	26.4	12.4
Plagioclase	39.3	46.5
Biotite	5.7	7.9
Amphibole	3.8	7.8
Pyroxene	—	0.8
Accessories	1.4	1.2
	100.0%	100.0%

the exsolved albitic feldspar is contained entirely within the borders of the potassic host. Exsolution in feldspars of the granodiorite takes the form of irregular and often diffuse patches, whereas in feldspars of the quartz monzonite, exsolution is more obvious, taking the form of lamellae and relatively large patches (Fig. 2). In many crystals the sodic phase is visibly twinned, usually according to the albite law. The general appearance of the perthites corresponds closely to the description of those from the Skye granites (Tuttle and Bowen, 1958, p. 103).

*Determinative techniques.* All optical work was done on a 4-axis Universal stage.  $2V$  was measured directly in sodium light by the extinction (orthoscopic) method to an accuracy of  $\pm 1^\circ$ . For each specimen,  $2V$  values were obtained for both phases of all suitably oriented perthite crystals in a single thin section and the values for the sodic phase and the potassic phase were tabulated separately. In the larger crystals, several  $2V$  values were obtained for each phase.

For  $x$ -ray work, hand specimens were crushed to pass a 120-mesh but

not a 230-mesh sieve, then alkali feldspar was separated by flotation in a bromoform-acetone mixture of density 2.585. This technique was effective in separating alkali feldspar from plagioclase, but traces of quartz remained in the float fraction. The excess quartz was detected in diffractometer patterns of the float fraction of more than half the samples. No attempt was made to further purify the samples after it was found that the alkali feldspar was fractionated in liquids of density less than 2.585. A single smear mount of each floated sample was made, then

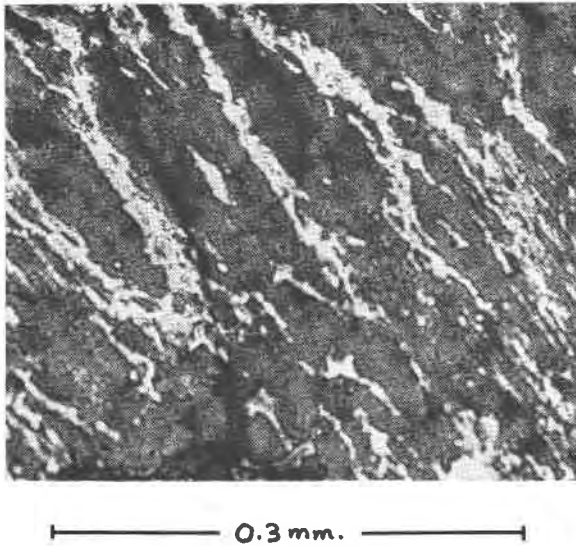


FIG. 2. Photomicrograph of a thin section of a typical micropertthite crystal from the quartz monzonite. Nicols crossed.

$x$ -rayed using filtered copper radiation from  $2\theta = 40^\circ$  to  $20^\circ$  at  $\frac{1}{2}^\circ$  min. The resulting  $x$ -ray diffractometer pattern was used to verify the perthitic nature of the alkali feldspar and to determine the obliquity of the potassic phase (MacKenzie, 1954).

A portion of each perthite sample was homogenized for two hours at  $1050^\circ$  C. in sealed platinum tube,  $\text{KBrO}_3$  was added as a standard (Orville, 1963) and the sample was then  $x$ -rayed using filtered copper radiation. Homogenization was tested by noting the sharpness of a peak at about  $2\theta = 21.1^\circ$  ( $\text{CuK}\alpha$ ) and the disappearance of the albite peaks at  $2\theta = 22.0^\circ$  and  $28.0^\circ$ . Bulk composition was obtained from Orville's (1963) curve relating Or content to the difference function  $2\theta$  ( $20\bar{1}$  feldspar)– $2\theta$  ( $110$   $\text{KBrO}_3$ ). To test the homogeneity of the initial sam-

ple two samples were homogenized on some specimens and the measured bulk compositions agreed to within 1 per cent Or, the limit of precision of the method.

Generally a quartz peak at  $26.6^\circ 2\theta$  was the only sign of impurity in the homogenized specimens. In some specimens this peak was joined by a quartz peak at  $20.8^\circ 2\theta$  whose intensity was no more than 10% of the adjacent  $20\bar{1}$  feldspar peak. Thus in the unhomogenized specimens interference of the feldspar  $20\bar{1}$  by quartz was considered to be negligible. On this basis the unhomogenized perthitic samples were run with  $\text{KBrO}_3$  as a standard and the composition of the potassium phase determined as above. Comparison of the relative compositions obtained in this way is justified by the low to negligible obliquity of the specimens and the fact that all the specimens are from the same plutonic body.

No attempt was made to obtain the composition of the sodic phase by means of the  $20\bar{1}$  spacing. Several authors have noted that the values of  $2\theta$  ( $20\bar{1}$ )  $-2\theta$  (standard) for this phase fall entirely off the published curves. The curves apply only to high-temperature Ca-free single phase alkali feldspar and the spacing is evidently affected by strain resulting from exsolution.

For single crystal study, samples were crushed to pass a 35-mesh but not a 120-mesh sieve. A small sample was then crushed further to obtain cleavage fragments of suitable size.

#### BULK COMPOSITION

Nine feldspars for which bulk composition was obtained from the  $20\bar{1}$  spacing were analyzed for  $\text{K}_2\text{O}$  and  $\text{Na}_2\text{O}$  by flame photometer, and for  $\text{CaO}$ ,  $\text{Al}_2\text{O}_3$  and  $\text{SiO}_2$  by  $x$ -ray fluorescence. The chemical data and the calculated feldspar compositions are given in Table 2. Figure 3 shows the comparison between bulk composition obtained by the two different methods. There is a systematic difference of 1–6 wt. % Or (average = 4%) with the analysis always indicating a lower value of

$$\frac{\text{Or}}{\text{Or} + \text{Ab} + \text{An}}$$

than that obtained by the  $x$ -ray method. The discrepancy, which decreases with increasing potassium content, is probably inherent in the two methods. Orville's (1963) curve is based on synthetic Ab-Or feldspars. It is evident that small amounts of  $\text{CaO}$ ,  $\text{BaO}$ ,  $\text{Fe}_2\text{O}_3$  and perhaps other material in the natural feldspars could produce a small shift of the  $20\bar{1}$  spacing. The differences are not considered important, because the main conclusions of this study depend on the  $x$ -ray measurement of the compositions of the potassic phases which lie in the range where the agreement is good.

TABLE 2. PARTIAL CHEMICAL ANALYSES<sup>1</sup> AND CALCULATED COMPOSITIONS OF SELECTED ALKALI FELDSPARS FROM THE TATOOSH PLUTON

Specimen Number	Quartz monzonite		Granodiorite						
	9	72	32	66	102	201	231	254	97
Na <sub>2</sub> O	2.49	2.18	1.52	1.81	1.79	1.96	2.39	2.89	2.50
K <sub>2</sub> O	12.3	12.9	13.8	13.2	13.2	13.7	12.1	11.0	11.8
CaO	0.55	0.50	0.42	0.48	0.49	0.55	0.49	0.55	≈0.5
Fe <sub>2</sub> O <sub>3</sub>	0.4	1.4	0.3	0.3	0.2	0.2	0.2	0.4	—
Al <sub>2</sub> O <sub>3</sub> (anal.)	19.2	19.0	18.3	17.6	18.9	17.8	18.0	18.4	—
Al <sub>2</sub> O <sub>3</sub> (calc.)	18.4	18.45	18.2	18.15	18.10	19.05	17.95	17.65	—
ΔAl <sub>2</sub> O <sub>3</sub>	+0.8	+0.55	+0.1	-0.55	+0.8	-1.25	+0.05	+0.85	—
SiO <sub>2</sub> (anal.)	66.0	65.5	65.7	66.0	66.0	65.3	65.4	66.1	—
SiO <sub>2</sub> (calc.)	62.7	63.2	62.7	62.1	62.1	65.2	61.5	60.2	—
ΔSiO <sub>2</sub>	+3.3	+2.3	+3.0	+3.9	+3.9	+0.1	+3.9	+5.9	—
Or	72.8	76.4	81.5	78.0	78.0	81.0	71.5	65.0	69.8
Ab	21.0	18.4	12.8	15.3	15.1	16.6	20.2	24.4	21.1
An	2.7	2.5	2.1	2.4	2.5	2.7	2.5	2.7	≈2.5
ΣOr+Ab+An	96.5	97.3	96.4	95.7	95.6	100.3	94.2	92.1	93.4
Or/Or+Ab+An (anal.)	75.5	78.5	84.6	81.5	81.5	81.0	75.9	70.5	74.9
Or% (x-ray) <sup>2</sup>	81.0	83.0	85.4	84.4	84.6	83.8	80.3	76.5	78.1
ΔOr%	5.5	4.5	0.8	2.9	3.1	2.8	4.4	6.0	3.2
An/Ab+An	11.4	11.9	14.1	13.5	13.9	14.0	10.8	9.9	—

<sup>1</sup> Flame photometer measurement of Na<sub>2</sub>O and K<sub>2</sub>O by J. I. Dinnin, U. S. Geological Survey. X-ray fluorescence measurement of CaO, Al<sub>2</sub>O<sub>3</sub>, SiO<sub>2</sub> and Fe<sub>2</sub>O<sub>3</sub> by H. J. Rose, Jr., U. S. Geological Survey.

<sup>2</sup> Method of Orville (1963). See text for details.

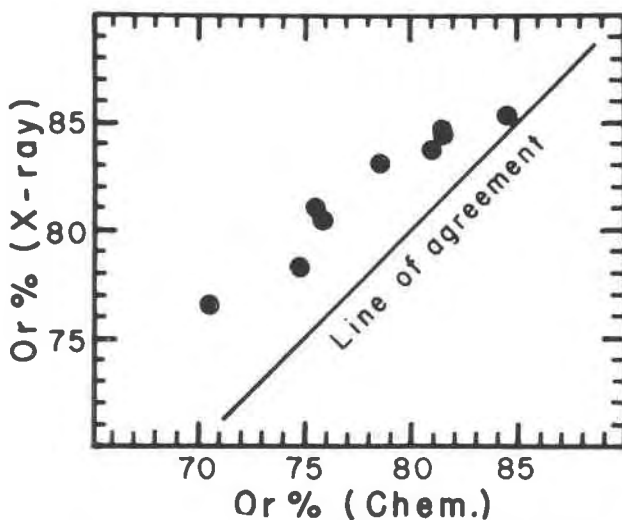


FIG. 3. Comparison of the bulk composition of perthites from the Tatoosh pluton obtained by two methods. The axis of the abscissa represents values of Or/Or+Ab+An (expressed as weight per cent) obtained from chemical analyses (Table 2). The axis of the ordinate represents values of Or/Or+Ab (expressed as weight per cent) obtained from measurement of the 20 $\bar{1}$  spacing of perthites homogenized at 1050° C. (Table 2).

Theoretical values of  $\text{Al}_2\text{O}_3$  corresponding to the ideal feldspar compositions have been computed from the  $\text{K}_2\text{O}$ ,  $\text{Na}_2\text{O}$  and  $\text{CaO}$  determinations. The calculated values generally fall within  $\pm 1\%$  of the  $\text{Al}_2\text{O}_3$  values obtained by  $x$ -ray fluorescence analysis (Table 2). The positive deviations may be caused by small amounts of argillitic alteration. The negative deviations can only be explained as errors in the analysis, since the low  $\text{Fe}_2\text{O}_3$  contents indicate that the feldspars are not alumina-deficient.

Theoretical values of  $\text{SiO}_2$  have also been computed and are compared in Table 2 with the  $\text{SiO}_2$  values obtained by  $x$ -ray fluorescence analysis. The differences ( $\Delta\text{SiO}_2$ ) ranging from (+) 0.1 to (+) 5.9 wt. % are a rough estimate of the quartz impurity in the samples. Another measure of the quartz content is given by the calculated value  $100\% - \sum \text{Or} + \text{Ab} + \text{An}$ . The two estimates are generally in close agreement ranging from no excess quartz (No. 201) to 6–8% excess quartz (No. 254). The agreement also demonstrates the internal consistency of the analyses.

#### POTASSIC PHASE

Table 3 summarizes the composition and obliquity of the potassic phase of the Tatoosh perthites.  $X$ -ray determination of bulk compositions is also given; the difference of Or content ( $\Delta E$ ) between the bulk composition and the composition of the potassic phase is a crude measure of the extent to which exsolution has proceeded. The values of  $\Delta E$  agree with qualitative estimates from thin sections of the amount of exsolution—the perthites in which exsolution shows up as weak and diffuse patches correspond to specimens with low values of  $\Delta E$ ; conversely the specimens with high  $\Delta E$  are perthites in which exsolution is marked by large patches and wide lamellae.

The  $2V$  measurements on the potassic phase are summarized in histograms (Fig. 4). Where  $2V$  could be measured on both the core and the rim of a crystal, both values are plotted, with a dot representing the value measured on the core. The mean  $2V$  for each specimen, including estimated mean values for the core-rim pairs, is plotted as a short vertical line. The average  $2V$  measured for each potassic phase is plotted against the composition of this phase in Fig. 5.

Most of the potassic phases are monoclinic to  $x$ -ray diffraction. Among these specimens  $2V$  increases in a general way with increasing potassium content (Fig. 5). Those specimens with average  $2V$  greater than about  $58^\circ$  and compositions more potassic than  $\text{Or}_{93}$  show broadening of the (130) and (131)  $x$ -ray diffraction peaks indicative of a triclinic lattice of variable small obliquity. The specimen having the highest  $2V$  (No. 211) is dominantly triclinic. The data regarding symmetry are summarized in Table 4. Thus with increasing potassium content the structural state

TABLE 3. NATURE OF THE POTASSIC PHASES OF PERTHITES FROM THE TATOOSH PLUTON

I. Quartz monzonite				
Specimen number	Bulk composition <sup>1</sup> (wt. % Or)	Potassic phase composition <sup>1</sup> (wt. % Or)	$\Delta E^2$ [Or (wt. %)]	(130) and (131) diffraction peaks
5	Or 84.2	Or 93.4	9.2	Slightly broad
9	81.0	91.7	10.7	Sharp
202	83.2	91.0	7.8	Sharp
13	81.6	92.0	10.4	Sharp
72	83.0	90.2	7.2	Sharp
152	80.0	90.2	10.2	Sharp
178	76.8	93.8	17.0	Broad
211	79.7	93.9	14.2	Broad
112	83.2	—	—	
237	83.8	94.0	10.2	Slightly broad
43	85.0	91.3	6.3	Sharp
44	85.4	90.0	4.6	Sharp
171	80.9	92.4	11.5	Sharp
Average	82.1	92.0	9.9	
II. Granodiorite				
231	Or 80.3	Or 91.0	10.7	Sharp
81	79.2	90.2	11.0	Sharp
25	86.0	90.7	4.7	Sharp
87	84.5	90.6	6.1	Sharp
32	85.4	89.4	4.0	Sharp
102	84.6	90.8	6.2	Sharp
64	80.6	89.5	8.9	Sharp
66	84.4	89.9	5.4	Sharp
74	84.7	89.3	4.6	Sharp
201	83.8	91.1	7.6	Sharp
254	76.5	91.0	14.5	Sharp
Average	82.7	90.3	7.6	

<sup>1</sup> Composition obtained from the position of the (20 $\bar{1}$ ) x-ray diffraction peak by the method of Orville (1963).

<sup>2</sup>  $\Delta E = [\text{Or (potassium phase)} - \text{Or (bulk)}]$ .

of the potassium phase shows a progressive deviation from orthoclase toward maximum microcline.<sup>1</sup>

The presentation in Fig. 5 differs from that used by other authors as

<sup>1</sup> The data of Fiorentini (1961) for perthites from a granitic intrusion show a similar relationship between Or content and structural state of the potassium phase.



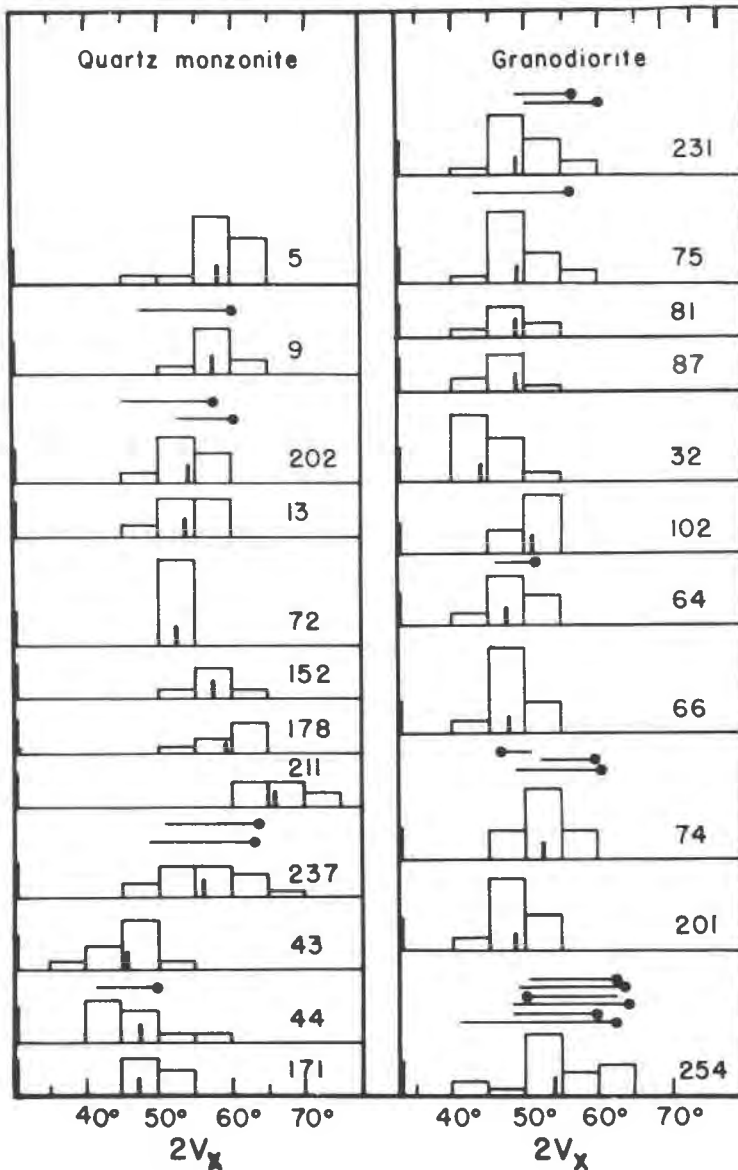


FIG. 4. 2V data for the potassic phase of perthites from the Tatoosh pluton. Each histogram, drawn for intervals of  $5^\circ 2V_x$ , summarizes measurements made on crystals in a single thin section. The height of the heavy bar at the left of each histogram represents five measurements. The specimen number is shown at the right. Measurements on the same crystal are connected by a horizontal line; a dot marks the measurement nearest the core of the crystal. The arithmetic average of the 2V's measured in one thin section is shown as a vertical bar in each histogram.

the  $2V$ 's are plotted opposite the composition of the potassic phase. In recent papers describing alkali feldspars (Tuttle and Keith, 1954; Tuttle and Bowen, 1958; Emeleus and Smith, 1959; Phair and Fisher, 1962)

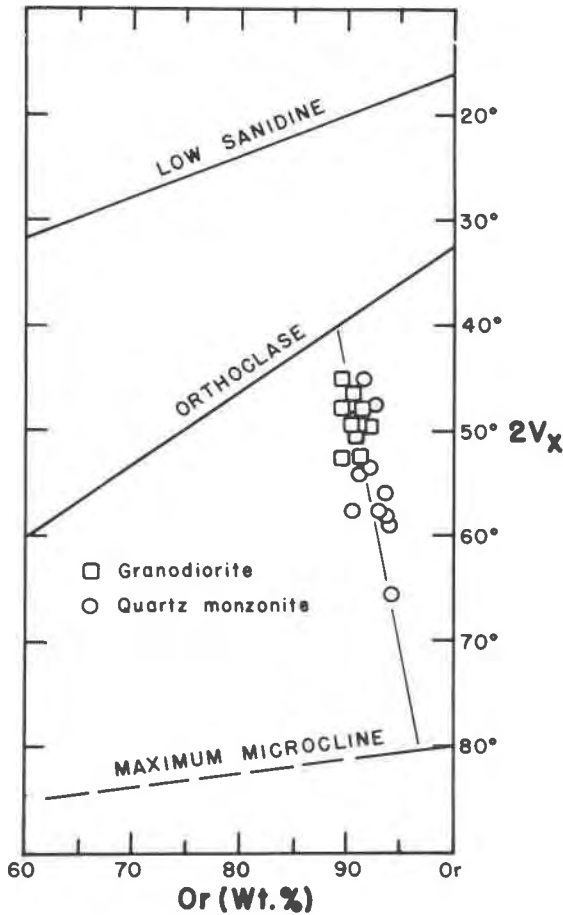


Fig. 5.  $2V$ -composition plot for the potassic phases of perthites from the Tatoosh pluton. Average  $2V$ 's are shown in Fig. 4; composition is given in Table 3.

$2V$  values are plotted above the bulk composition of the feldspar on a graph of  $2V$  vs composition.

This difference in the method of plotting arises from a fundamental distinction between micro- and crypto-perthites. As used by most authors cryptoperthite is applied to alkali feldspars in which exsolution may be detected only by  $x$ -ray diffraction, whereas microperthite implies that

exsolution is visible in thin section.<sup>1</sup> Although these terms are in common use, authors who summarize optical measurements on perthites do not always indicate clearly what kind of perthite is being measured. The importance of such a distinction is this: 2V measurements on crystals in which no exsolution can be detected optically obviously reflect some

TABLE 4. SINGLE CRYSTAL DATA FOR THE PERTHITES FROM THE TATOOSH PLUTON

Rock Unit	Spec. No.	Symmetry of Potassium Phase	Sodium phase				
			Twinning	$\alpha^*$	$\gamma^*$	I	Character of spots
Granodiorite	32	Monoclinic	Albite	86°31'	89°16'	Weak	Very diffuse
	102	Monoclinic	Albite	86°21'	89°48'	Weak	Diffuse
	66	Monoclinic	Albite Pericline	86°22' —	89°16' —	Weak	Diffuse
	201	Monoclinic	Albite Pericline	86°18' —	89°27' —	Weak	Diffuse
	254	Monoclinic	Albite twin-type superstructure			Fairly Strong	5 spots: 3 sharp and 2 diffuse
Quartz monzonite	72	Monoclinic	Albite Pericline	86°35' —	89°30.5' —	Strong Weak	Fairly sharp
	9	Monoclinic	Albite	86°26'	89°42'	Strong	Sharp spots
	5	Dominantly monoclinic with triclinic phase of variable, small obliquity <sup>1</sup>	Albite Pericline	86°25' —	89°50' —	Strong Weak	Sharp —
	211	Dominantly triclinic <sup>2</sup> with variable obliquity.	Albite Pericline	86°24' —	90°00' —	Strong Weak	Sharp —

<sup>1</sup> Estimated maximum obliquity:  $\alpha^* = 90^\circ 05'$ ;  $\gamma^* = 90^\circ 10'$ .

<sup>2</sup> Angles for potassium rich phase:  $\alpha^* = 90^\circ 15'$ ;  $\gamma^* = 91^\circ 16'$ .

*bulk* property of the crystal, although not necessarily one that is simply related to composition (see below). As soon as the separation of another phase can be detected under the microscope two sets of optical measurements are necessary to describe the crystal—a set corresponding to each phase. As long as two sets of 2V values can be measured it is obvious that they cannot be combined in any simple way to reflect a property

<sup>1</sup> See the distinction between micro- and crypto-perthite given in MacKenzie and Smith, 1955, p. 708.

dependent on the bulk composition of the perthite. In measurements made on microperthites, then, the set of 2V measurements on the potassium-rich host must be equated with the composition of *that* phase if it is to have any meaning at all.

One reason why this idea has been overlooked in the recent literature stems from statements made originally by Spencer (1937) in connection with heating experiments on perthites. One of Spencer's conclusions from short heating runs (1–2 hrs.) at 800° is that when megascopic exsolution lamellae visible at the start of the experiment were redissolved, there was little or no change in 2V. This has been interpreted by recent authors to imply the reverse—that is, the 2V of an initially homogeneous alkali feldspar does not change with exsolution.<sup>1</sup> Since Spencer's experiments were performed dry and without *x*-ray confirmation of either homogenization or possible partial conversion to sanidine, the author feels that Spencer's results are inconclusive with respect to the changes in 2V resulting from exsolution.

2V measurements made on cryptoperthites can be influenced both by composition and by possible variations in the structural state of the exsolved phases. For example, Tuttle and Bowen (1958) attribute variations in 2V to changes in the relative amounts of sub-microscopically exsolved high and low albite. Because 2V may be affected by both bulk composition and by parameters which are independent of composition the significance of 2V correlated with bulk composition is ambiguous.<sup>2</sup> For several reasons, then, the method of plotting 2V opposite the bulk composition on a 2V-composition diagram should be abandoned for all perthitic feldspars.

The question remains whether, in microperthites, the optically homogeneous areas in the host could not be cryptoperthitic. For the Tatoosh perthites the existence of cryptoperthite is unlikely. Exsolution shows up optically as numerous patches, even in the perthites for which  $\Delta E$  is small and for which the strong peak for the sodic phase is hardly visible on an *x*-ray diffraction pattern. This indicates that exsolution lamellae become visible very soon after unmixing begins and that the optically homogeneous areas in the host must consist essentially of a single phase.

<sup>1</sup> MacKenzie and Smith (1955, p. 708–9) make the statement: "To name a particular alkali feldspar using [Tuttle's] curves, it is not necessary to know whether or not the feldspar is unmixed, the optic angle being that of either a homogeneous crystal or the aggregate affect produced by the intergrowth of the separate phases."

<sup>2</sup> If it is accepted that 2V cannot be correlated with bulk composition, then the contention of Tuttle and Bowen (1958), on the basis of their 2V data, that feldspars intermediate between sanidine and orthoclase exist is open to question. At least one cannot demonstrate from 2V data alone that there are structurally intermediate members analogous to the orthoclase-microcline relations documented in this paper and elsewhere.

## SODIC PHASE

The range of  $2V$  measurements on the sodic phases are presented in Fig. 6. Most specimens have an exceptionally wide range of values, even if only the  $2V$  values measured on sodic blebs in a single perthite crystal are considered. The spread of  $2V$ 's indicates that the sodic phase has a range of structural state<sup>1</sup> between high albite ( $2V_x = 45^\circ$ ) and low albite ( $2V_x = 103^\circ$ ). The  $2V$  of the sodic phase was found to depend on the size of the sodic bleb, as illustrated by specimen number 66 (Fig. 6) and by

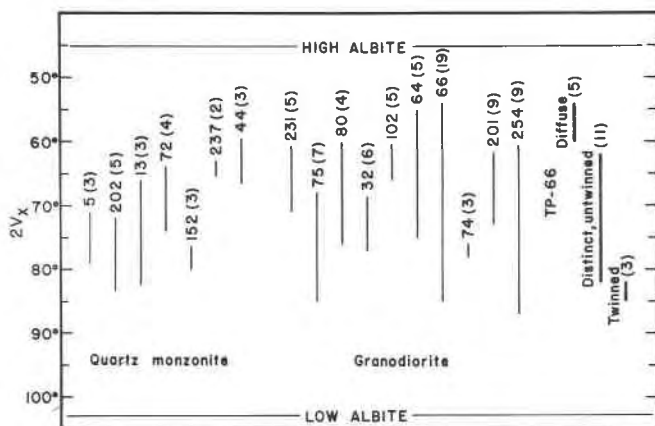


FIG. 6.  $2V$  data for the sodic phase of perthites from the Tatoosh pluton. The range of  $2V$  for each specimen is given by a vertical bar. The specimen number with the number of measurements in parenthesis are written above the bar; e.g. 201 (9). The  $2V$  range for specimen number 66 is broken down at the right according to the appearance of the exsolution patches. See text and also Fig. 7 for further explanation.

specimen number 254 (Fig. 7). Where blebs are diffuse, untwinned and can only be distinguished from the host by a slightly higher birefringence, the  $2V$ 's are low (55–65, rarely 50–55). Where the blebs are well defined but still untwinned, the  $2V$ 's usually fall in the 65–80° range. Twinned blebs generally give even higher values (80–85°). Thus within a single grain of perthite there appears to be a correlation among the following three properties:

1. Increased definition and size of exsolution blebs.
2. Increased  $2V$  values.
3. More highly developed twinning.

The magnitude of  $2V$  is again provisionally correlated with differences in structural state. Grain size of the exsolution blebs may influence the

<sup>1</sup>  $2V$  may be affected by differences in composition but this effect is small compared to the effect of structural state.

2V directly but neither the sense nor magnitude of such an effect is known.

Oscillation photographs around the  $b$ -axis were taken of several alkali feldspar crystals in the standard orientation proposed by Smith and MacKenzie (1955). The data obtained for the sodic phase are summarized in Table 4. The reciprocal lattice angles  $\alpha^*$  and  $\gamma^*$ , obtained by the procedure outlined by Smith and MacKenzie, are plotted in Fig. 8. Most specimens have a sodic phase twinned on the albite or albite and pericline

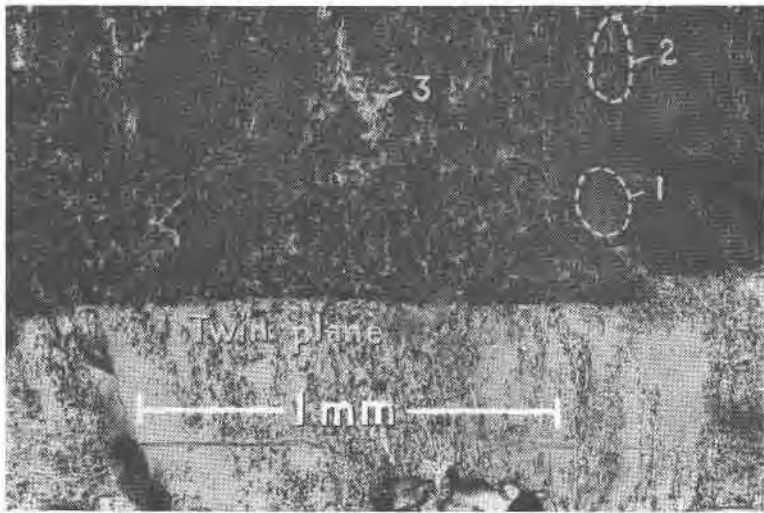


FIG. 7. Photomicrograph of a thin section showing different stages of exsolution in a perthite. On one side of the twin the potassic host is dark and the sodic exsolution patches are light. The variation of  $2V$  with size of exsolution patches is as follows: Nicols crossed.

1. Exsolved albite barely resolvable by means of higher birefringence  $2V_x = 57^\circ$ .
2. Small lamellae  $2V_x = 70^\circ$ .
3. Large untwinned patch.  $2V_x = 76^\circ$ .

laws. One crystal gives a pattern similar to that interpreted by Smith and MacKenzie as due to an "albite-twin type superstructure"; the bulk composition ( $\text{Or}_{70}\text{Ab}_{30}$ ) of this specimen lies with the range  $\text{Or}_{75}\text{--}\text{Or}_{60}$  predicted by MacKenzie and Smith for the development of this twin type.

Figure 8 shows, in addition to the data in Table 4,  $\alpha^*\text{--}\gamma^*$  pairs for sodium-rich feldspars of known structural state and composition. Plagioclases of low structural state are characterized by a strong dependence of  $\gamma^*$  on An content. This not so for plagioclases of high structural state; as shown by Smith (1956) high plagioclases of composition

An<sub>0</sub>-An<sub>50</sub> all plot very close to position of high albite in Fig. 8. Low albites, having An contents of up to 11%, from orthoclase and microcline perthites studied by MacKenzie and Smith (1955) plot within the hatched area. The displacement of these from the position of low albites

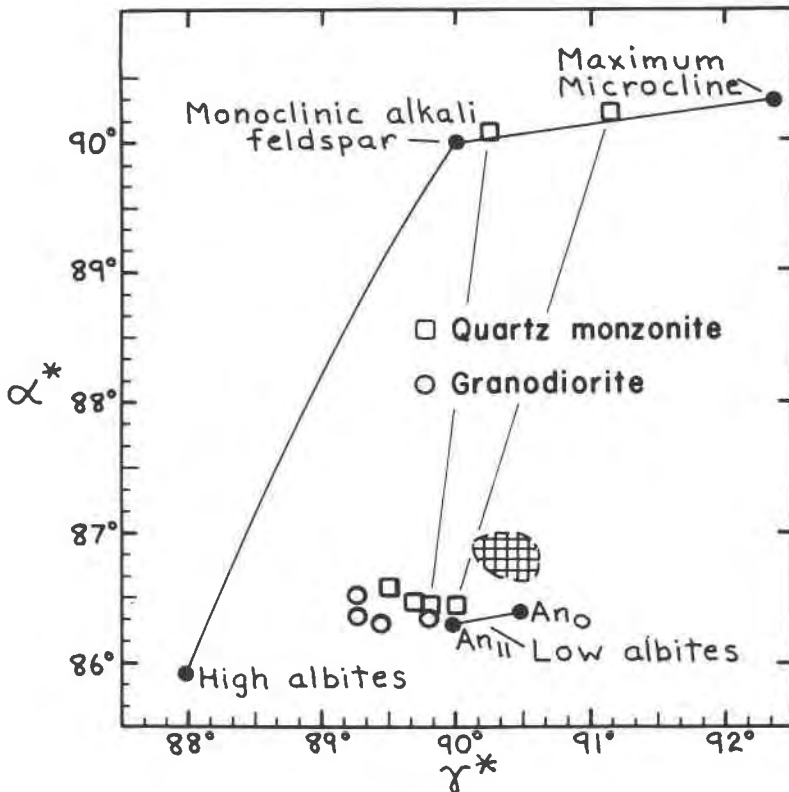


FIG. 8. Plot of the reciprocal lattice angles  $\alpha^*$  and  $\gamma^*$  of the sodic and potassic phases of perthites from the Tatoosh pluton (Table 4). The solid circles are data from MacKenzie and Smith (1955). The cross-hatched area covers the range of  $\alpha^*$ - $\gamma^*$  pairs for the sodic phase of orthoclase and microcline perthites studied by MacKenzie and Smith (1955, 1962).

of equivalent composition not occurring in perthitic intergrowth is probably the result of strain accompanying exsolution. The sodic phases of the Tatoosh perthites, with maximum An contents of 10-14% (Table 2), are clearly of intermediate structural state as compared with the specimens studied by MacKenzie and Smith. The structural state of the sodic phase is closer to low albite in specimens which show greater exsolution and which have a potassic phase of higher obliquity (Fig. 8).

## EXSOLUTION AND INVERSION HISTORY OF THE TATOOSH PERTHITES

The data presented suggest that both phases of the perthites have undergone a continuous second-order change from a higher to lower structural state during exsolution. Two models of the phase relations on the binary Or-Ab solvus may be formulated to explain these relations, the choice of one over the other depending on whether the data are presumed to reflect equilibrium or disequilibrium cooling at subsolidus temperatures. These models, similar in form to those proposed by Wones

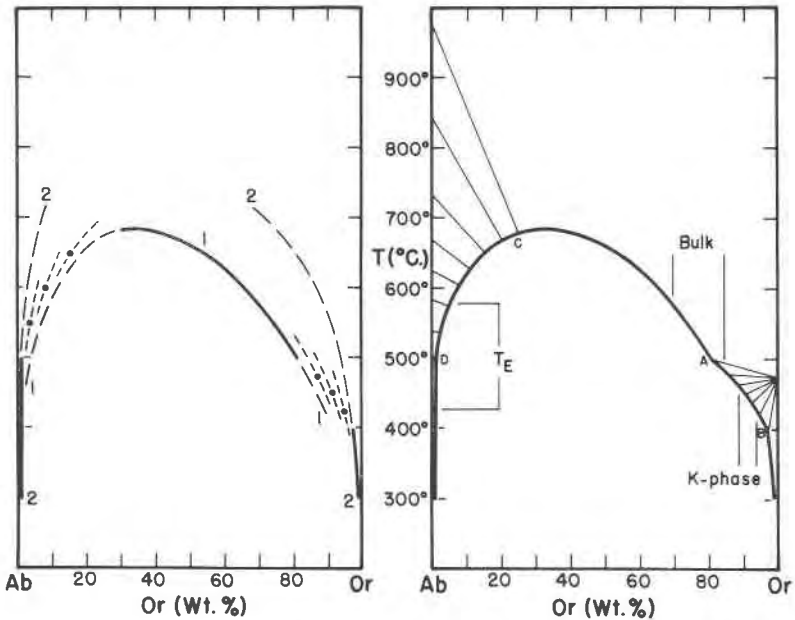


FIG. 9. Phase relations in the Ab-Or system at low temperatures assuming second order transitions for both phases crystallizing on the solvus. (a) Method of constructing the solvus; (b) completed solvus with lines bracketing the bulk composition (BULK), potassium-phase composition (K-phase) for the Tatoosh perthites, and the range of temperatures ( $T_E$ ) during exsolution. See text for further explanation.

and Appleman (1963), have been constructed using experimental determination of the solvi for both ordered and disordered alkali feldspars and the compositions of the Tatoosh feldspars so that the exsolution process can be discussed in at least a semiquantitative fashion.

The first model, which assumes that the Tatoosh data reflect equilibrium cooling, is shown in Fig. 9b, constructed as indicated in Fig. 9a. The solvus labeled "1" in Fig. 9a is that determined by Orville (1963)



for synthetic sanidines crystallized at 2000 bars total pressure in the presence of 2M alkali chloride solution. The portion of this solvus which is assumed here to be stable is drawn as a heavy solid line—metastable extensions are dashed toward lower temperatures. The solvus labeled "2" in Fig. 9a is a hypothetical solvus for the low albite-maximum microcline series. Orville (writt. comm., 1963) indicates that this solvus lies everywhere outside the sanidine solvus and is positioned approximately as shown. The stable solvus is drawn as two heavy solid lines with metastable extensions dashed toward higher temperatures. Between these two limiting solvi, defined by feldspars of maximum high and maximum low structural state, an infinite number of intermediate solvi could exist, each corresponding to a feldspar having a fixed intermediate structural state. Three such solvi are shown; each would be stable at two points of fixed temperature and composition from which metastable extensions extend toward both higher and lower temperatures.

The composite solvus, representing feldspars coexisting in equilibrium at constant pressure is shown in Fig. 9b. The points A and B, between which the stable potassium feldspar is of intermediate structural state, are placed so as to bracket the range of composition found for the potassic phase of the Tatoosh perthites. The analogous points on the Ab side of the diagram, C and D, are arbitrarily placed as no estimate of the composition of the sodic phase of the Tatoosh perthites is available. Between A-B and C-D, the second-order structural transitions are shown by lines of equal Al-Si order ranging between complete disorder (uppermost line) to complete order (lowermost line). The extrapolation of these lines to the Or and Ab sidelines is based on an evaluation of previous work on the nature of the structural transformations in the pure feldspars. These interpretations are in no way suggested or reinforced by data of the present study. The continuous transition at the Ab sideline was suggested by MacKenzie (1957) from syntheses of apparently stable intermediate albites in long runs at constant temperature. MacKenzie placed the temperature limits of the transition at approximately 1000° and 450° C. for pressures of 1000–2000 bars. The convergence of the order lines to a first-order transition at the Or sideline is suggested by hydrothermal heating experiments of Goldsmith and Laves (1954) and Tomisaka (1962) which show a conversion of maximum microcline to a monoclinic feldspar at temperatures above about 500° without intervention of intermediate structural states. The interpretation of a first-order transition is favored by Wones and Appleman (1963) by analogy with their determination at 2000 bars total pressure of a reversible transformation of synthetic iron-sanidine to iron microcline at  $704^{\circ} \pm 6^{\circ}$  C.

A possible history of exsolution and inversion of the Tatoosh perthites can now be formulated with the aid of Fig. 9b. Feldspars of bulk composition  $Or_{76}-Or_{85}$  began exsolving at temperatures of 550–500° C. and completed exsolution at temperatures of 460–430° C., corresponding to the range in potassic-phase composition of  $Or_{89}-Or_{94}$ . During exsolution the potassic phase underwent continuous change toward a lower structural state; the final composition and structural state for each perthite reflects the temperature at which exsolution ceased.

The range of structural state observed for the sodium phase is difficult to interpret in analogous fashion as representing equilibrium; the temperatures of completion of exsolution derived from the composition of the potassic phase lie within the presumed stability field of low albite. It is likely that the sodic phase separated initially as metastable high albite and did not invert completely during exsolution. This interpretation is favored by the observation of a range of structural states in a single perthite crystal, a condition inconsistent with attainment of equilibrium.

The preceding discussion has assumed that the potassic phases of the Tatoosh perthites were at equilibrium during exsolution. If this assumption is discarded then the possibility of a first-order transition on the solvus must be considered. A model of the phase relations, assuming a first-order transition, is shown in Fig. 10. This model is suggested by data on the inversion of maximum microcline to orthoclase in perthites affected by contact heating in the vicinity of a granitic stock (Hart, in press). Hart describes the transition as occurring over an interval of less than 100 feet in perthites collected 1100 feet from the nearest contact of the stock. Further study being made by D. R. Wones and the present author shows that the change of symmetry is accompanied by an abrupt increase in the sodium content of the potassic phase. The diagram has been completed by connecting the first-order transition on the solvus to a first-order transition on the Or sideline by means of a transition loop. There are other possible configurations but data are not yet available to evaluate the possibilities and choose among them. If Fig. 10 is assumed to represent the equilibrium phase relations, then the Tatoosh feldspars represent metastable stages in the conversion of orthoclase to maximum microcline at temperatures below the equilibrium temperature of transition. An orthoclase cooled through the transition should, if equilibrium prevailed, invert rapidly and completely to maximum microcline at the transition temperature. If reaction rates were too slow to reach equilibrium then the orthoclase might invert along a metastable path such as that dashed in Fig. 10. Along the path shown the composition of the

potassic phase would become more potassic as inversion proceeded in agreement with the data in Fig. 5. Other metastable paths are possible, depending on the stable phase relations above the transition temperature. For example, a feldspar could follow a cooling path lying on or between

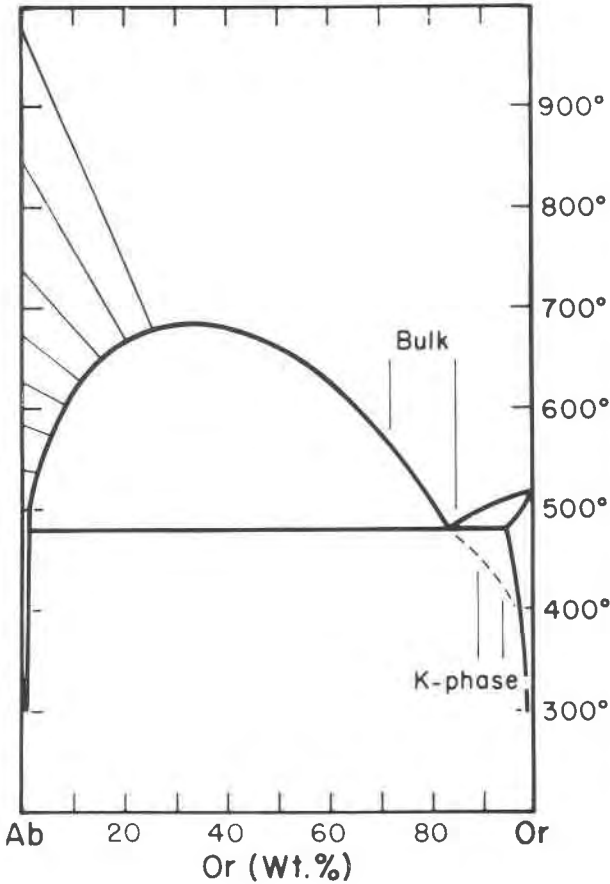


FIG. 10. Phase relations in the Ab-Or system at low temperatures assuming a first-order transition for the potassic phase of a perthite crystallizing on the solvus. Legend as in Fig. 9b.

metastable extensions of the transition loop shown in Fig. 10 but this would require that the potassic phase(s) become more sodic with falling temperature.

From the present study alone it is not possible to judge whether exsolution is an equilibrium or disequilibrium process. Extrapolation of

the data suggests that the stable potassic feldspar at low temperatures is maximum microcline and that exsolution of any homogeneous feldspar crystallized above the Or-Ab solvus should, with extended cooling, produce a perthite in which maximum microcline more potassic than Or<sub>96</sub> and low albite of negligible Or content would be the stable phases.

#### ACKNOWLEDGMENTS

This study represents part of a doctoral dissertation submitted to Johns Hopkins University. I would like to thank Hans Eugster, who supervised the work presented here, and A. C. Waters, who offered additional helpful criticism and discussion. D. B. Stewart, D. Appleman, P. Toulmin and F. W. Cater, all of the U. S. Geological Survey, critically reviewed the manuscript. Their many improvements are gladly acknowledged. W. S. MacKenzie and I. D. Muir also reviewed an earlier version of the manuscript and gave many helpful suggestions both as to presentation and interpretation of the data. Finally, I would like to acknowledge communications from D. R. Wones, O. F. Tuttle, C. H. Emeleus and J. V. Smith, all of whose ideas have been most welcome.

#### REFERENCES

- EMELEUS, H. AND J. V. SMITH (1959) The alkali feldspars. VI. Sanidine and orthoclase perthites from the Slieve Gullion Area, Northern Ireland. *Am. Mineral.* **44**, 1187-1209.
- FIorentini, POTENZA M. (1961) Evoluzione strutturale, Dispersione Ottica ed Altri Caratteri del K-Feldspato nelle zone differenziate della massa intrusiva della valle del cervo. *Rend. Inst. Lombardo Acc. Sci. e Lettere, Milan*, **95**, 807-826.
- GOLDSMITH, J. R. AND F. LAVES (1954) The microcline-sanidine stability relations. *Geochim. Cosmochim. Acta*, **5**, 1-19.
- HART, S. R. The petrology and isotopic mineral age relations of a contact zone in the Front Range, Colorado. *Jour. Geol.*
- MACKENZIE, W. S. (1954) The orthoclase-microcline inversion. *Mineral. Mag.* **30**, 354-366.
- (1957) The crystalline modifications of NaAlSi<sub>3</sub>O<sub>8</sub>. *Am. Jour. Sci.* **255**, 481-516.
- AND J. V. SMITH (1955) The alkali feldspars. I. Orthoclase microperthites. *Am. Mineral.* **40**, 707-732.
- AND J. V. SMITH (1962) Single crystal x-ray studies of crypto- and micro-perthites. *Norsk Geol. Tidssk. (feldspar volume) B.* **42**, 72-103.
- ORVILLE, PHILIP M. (1963) Alkali ion exchange between vapor and feldspar phases. *Am. Jour. Sci.* **261**, 201-237.
- PHAIR, G. AND F. G. FISHER (1962) Laramide comagmatic series in the Colorado Front Range: The feldspars. *Geol. Soc. Am. Bull. Buddington Vol.*, 479-522.
- SLEMMONS, D. B. (1962) Determination of volcanic and plutonic plagioclases using a three- or four-axis universal stage. *Geol. Soc. America Spec. Paper* **69**.
- SMITH, J. V. (1956) The powder patterns and lattice parameters of plagioclase feldspars. I. The soda-rich plagioclases. *Mineral. Mag.* **31**, 47-68.
- AND W. S. MACKENZIE (1955) The alkali feldspars. II. A simple x-ray technique for the study of alkali feldspars. *Am. Mineral.* **40**, 733-747.

- SPENCER, E. (1937) The potash-soda feldspars. I. Thermal stability. *Mineral. Mag.* **24**, 453-494.
- TOMISAKA, T. (1962) On order-disorder transformation and stability range of microcline under high water vapor pressure. *Mineral. Jour.* [Japan] **3**, 261-281.
- TUTTLE, O. F. AND N. L. BOWEN (1958) Origin of granite in the light of experimental evidence in the system Or-Ab-SiO<sub>2</sub>-H<sub>2</sub>O. *Geol. Soc. Am. Mem.* **74**.
- AND M. L. KEITH (1954) The granite problem. Evidence from the quartz and feldspar of a Tertiary granite. *Geol. Mag.* [Gt. Brit.] **91**, 61-72.
- WONES, D. R. AND DANIEL APPLEMAN (1963) Properties of synthetic triclinic KFeSi<sub>3</sub>O<sub>8</sub>, iron microcline, with some observations on the iron microcline⇌iron sanidine transition. *Jour. Petrol.* **4**, 131-137.

*Manuscript received, October 10, 1963; accepted for publication, February 27, 1964.*